World Scientific
www.worldscientific.com

Ag$_2$S–CoS$_2$ hetero-nanostructures: One-pot colloidal synthesis and improved magnetic properties

Yuanjun Liu and Aihua Yuan*
School of Biology and Chemical Engineering
Jiangsu University of Science and Technology
Zhenjiang 212018, P. R. China

Guoxing Zhu[†], Chunlin Bao, Rongxian Zhang and Xiaoping Shen
School of Chemistry and Chemical Engineering
Jiangsu University, Zhenjiang 212013, P. R. China
*aihuayuan@163.com
†zhuguoxing@ujs.edu.cn

Ag$_2$S–CoS$_2$ hetero-nanostructures with well defined and sharp hetero-interface were synthesized with a simple one-pot colloidal chemical route. It is proposed that the Ag$_2$S nanoparticles with superionic conductor properties play a catalyst role inducing the growth of CoS$_2$. The magnetic properties of the Ag$_2$S–CoS$_2$ hetero-nanostructures were investigated, which gives a saturation magnetization of 8.3 emu/g at 1.8 K and transition temperature of 120 K. It is believed that the reported results would give some hints to the development of multifunction magnetic materials.

Keywords: Hetero-nanostructures; CoS$_2$; magnetic properties; Ag$_2$S; superionic conductor.

Integrating two or more different compositions into one micro-/nanostructure forming nanocomposites is highly considered to be one of the effective routes for developing new functional materials. This integration will not only combine the excellent properties or functions from different compositions into one micro-/nanostructure, but also often induce new performances, which are not present in their individual nanounits.[1,2] Combining several nanounits into complex nanosystems is also a key step for the application of various nanomaterials in devices. Due to the flexibility of bandgap engineering, semiconductor–semiconductor or metal-semiconductor nanostructures have been considered to offer better opportunities for internal exciton separation, carrier transport and opto-electronic applications.[3,4]

The usual route for the fabrication of these hetero-nanostructures is seed-assistant method. In this case, the second material grows epitaxially on the seed.[5,6] Thus, the second material has well-defined orientation with respect to the seed crystal structure. The whole particle containing two or more compositions seems to be a single crystal. The bigger lattice energy makes the hetero-nanostructure be stable. However, the control of the heteroepitaxy is still a challenge at present stage, especially in solution conditions, because the second materials often self-nucleate and grow.[7] Recently, Gao *et al.* reported that Cu$_{1.94}$S can induce the growth of In$_2$S$_3$ through a defect mediated process forming Cu$_{1.94}$S–In$_2$S$_3$ hetero-structures.[8] We also found that superionic conductor Ag$_2$S can be used as a unique medium for the growth of semiconductor, forming Ag$_2$S–ZnS, Ag$_2$S–CdS hetero-structures with epitaxial hetero-interface.[9] Up to date, several cases of semiconductor–semiconductor hetero-structures have been reported including Cu$_2$S–CuInS$_2$,[10] Cu$_2$S–CdS,[11,12] Cu$_2$S–PbS.[13]

CoS$_2$ has attracted much attention for a long time due to its potential application in spin-electronic devices.[14,15] It is a metallic ferromagnet with a curie temperature of about 120 K.[16,17] CoS$_2$ with pyrite structure also shows excellent conductivity and promising catalytic performance for the oxygen reduction reaction.[18,19] In addition, it has good stability in acid media, higher thermal stability (decomposition temperature above 650°C), and lower solubility in molten electrolyte.[20] These allow its long-term application in various fields such as Li-ion batteries and supercapacitors. Up to now, several methods have been successfully designed to fabricate CoS$_2$ micro-/nanostructures.[21] However, no report is on the fabrication of CoS$_2$-based hetero-structures with epitaxial

---

†Corresponding author.

Y. Liu et al.

hetero-interface. Therefore, the driving force of this study is to extend the catalytic route for the synthesis of Ag_2S–CoS_2 hetero-structures and to determine whether the formation of hetero-structures has influence on their magnetic properties. Here, Ag_2S–CoS_2 hetero-structures were synthesized by thermal co-decomposition of the precursors, $AgNO_3$ and Co(dbdc)$_2$ (dibutyldithiocarbamate, dbdc), which is much more convenient than the multi-step seed-assistant method.

All reagents were used as received without further purification. The Co(dbdc)$_2$ precursor was synthesized with a reported route.[22] In a typical synthesis of Ag_2S–CoS_2 hetero-structure, 4.0 g of octadecylamine was added in an opened flask, which was heated at 170°C and kept at this temperature for 20 min with stirring to get rid of volatile impurities in it. Then, 36 mg of $AgNO_3$ and 50 mg of sulfur powder was added orderly. After reaction for about 10 min, the reaction system turned to be black, indicating the formation of Ag_2S nanoparticles. 120 mg of Co(dbdc)$_2$ was then slowly added (by adding 20 mg of Co(dbdc)$_2$ every 5 min) under stirring and reaction for about 60 min at 170°C. The products were collected by centrifugation and thoroughly washed with *n*-heptane, $CHCl_3$ and ethanol.

For crystal phase identification, the obtained powder sample was examined with a X-ray powder diffractometer (XRD, CuK$_\alpha$ radiation, Bruker D8 advance diffractometer, $\lambda = 1.5406$ Å). The morphologies and dimensions of the samples were investigated using a JEOL-2100 high-resolution transmission electron microscope (HR-TEM) with accelerating voltage of 200 kV. The magnetic properties of the obtained Ag_2S–CoS_2 hetero-structures were investigated with a Quantum Design MPMS XL-7 superconducting quantum interference device (SQUID).

XRD technique was first used to detect the phase and composition of the product. The corresponding XRD pattern is shown in Fig. 1. The peaks can be indexed into the mixture of monoclinic phase Ag_2S (JCPDS No. 14-0072) and cubic phase CoS_2 (JCPDS No. 41-1471), which suggests that Ag_2S
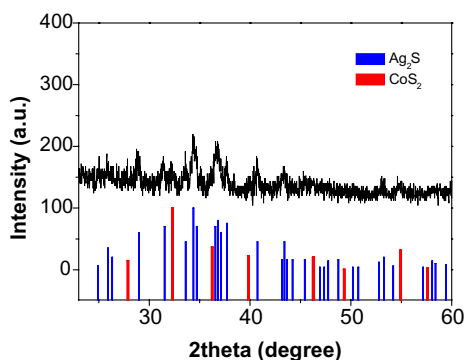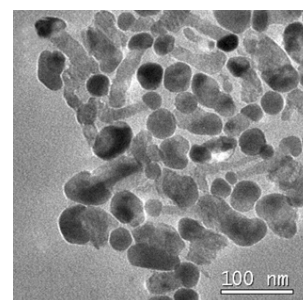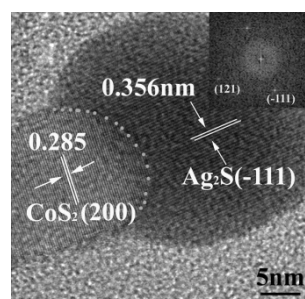
and CoS_2 formed in the reaction. No impurities such as Ag are detected.
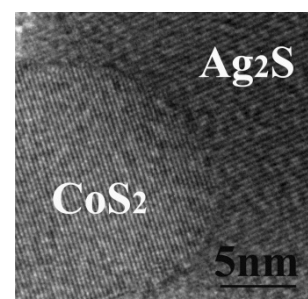
The morphology and microstructure of the Ag_2S–CoS_2 hetero-structures were then determined by a JEOL-2100 transmission electron microscope (TEM). The TEM images are shown in Fig. 2, which demonstrates a "match-like" structure. On one end of the nanorod, a particle with deeper contrast was observed. The particles have the size of 10–40 nm, while the rods have lengths of 60–90 nm with diameters of 15–30 nm. The different contrast of the particle and the rod indicates that the "match-like" structures are composed of two compositions (Ag_2S, CoS_2). This is further confirmed with HR-TEM analysis. Figures 2(b) and 2(c) show HR(-)TEM images recorded on the junction between the nanoparticle and the nanorod. Clear lattice fringes are observed for both areas. For the particle, the lattice fringe
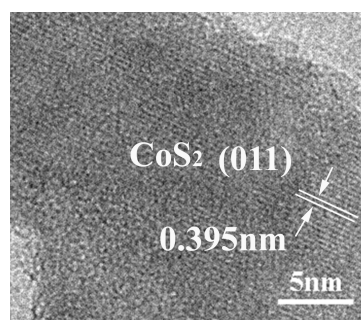

(a)

(b)

(c)

Fig. 1. XRD pattern of Ag_2S–CoS_2 hetero-structure. Standard patterns of Ag_2S (JCPDS No. 14-0072) and CoS_2 (JCPDS No. 41-1471) were also shown with blue and red color for comparison.
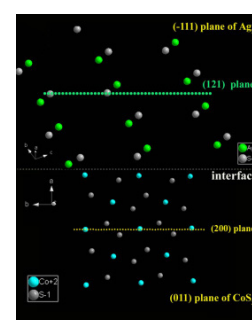

(d)

(e)

Fig. 2. (a) TEM, (b)–(d) HR(-)TEM images of the prepared Ag_2S–CoS_2 hetero-structures and (e) schematic image of the hetero-interface.

spacing is 0.356 nm, corresponding to the (−111) crystal plane of monoclinic Ag$_2$S. The lattice spacing recorded on the rod is 0.320 nm, which is attributed to the (200) crystal plane of cubic CoS$_2$ phase. Thus it is concluded that the CoS$_2$ nanorods grow along the (200) direction. The corresponding fast Fourier transform (FFT) pattern of the Ag$_2$S area is shown in the inset of Fig. 2(b), which suggests the (121) lattice plane of Ag$_2$S is parallel to the (200) lattice plane of CoS$_2$. The composition of the product was further determined by an Energy dispersive spectrograph equipped on the TEM, which shows the existence of Ag, Co, S elements.

The interface between Ag$_2$S and CoS$_2$ is sharp and regular, but with arc shape (Figs. 2(b) and 2(c)), suggesting that CoS$_2$ grows from Ag$_2$S catalyst, but not the case that it directly grows on the surface of Ag$_2$S. Thus the role of Ag$_2$S in the growth process is a catalyst, not a seed.[9] The seed only provides a surface platform for the growth of material, but don't have shape or size change in the process.

For the analysis of the lattice mismatch status between Ag$_2$S and CoS$_2$, a further HR(-)TEM observation was carried out. Figure 2(d) provides the HR(-)TEM image of CoS$_2$ nanorods with lattice fringes vertical to the hetero-interface. The corresponding fringe with spacing of 0.395 nm is originated from the (011) crystal plane of cubic CoS$_2$ phase. The mismatch between (011) crystal plane of cubic CoS$_2$ and (−111) crystal plane of monoclinic Ag$_2$S is 9.9%. The formation of the hetero-interface with higher lattice mismatch can be attributed to the unique catalyst-assisted growth mechanism. Based on these, a schematic image of the hetero-interface was shown in Fig. 2(e).

We then investigated the influence of the reaction parameters on the formation of Ag$_2$S–CoS$_2$ hetero-structure. With smaller amount of Co(dbdc)$_2$, Ag$_2$S–CoS$_2$ hetero-structure with smaller volume of CoS$_2$ is obtained. For example, with 50 mg of Co(dbdc)$_2$, as shown in Fig. 3(a), only smaller volume of CoS$_2$ formed in the nanoparticles. Decreasing the growth temperature of CoS$_2$ to 150°C does not have obvious influence on the formation of hetero-structure under given situations. It should be noted that the adding of
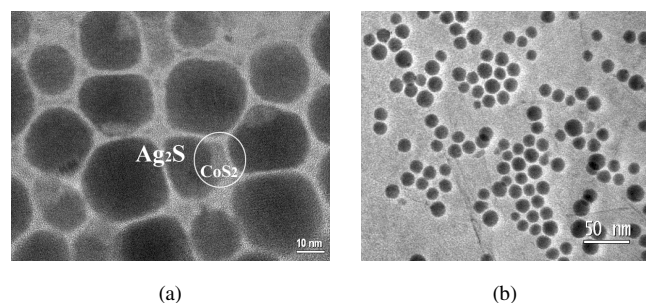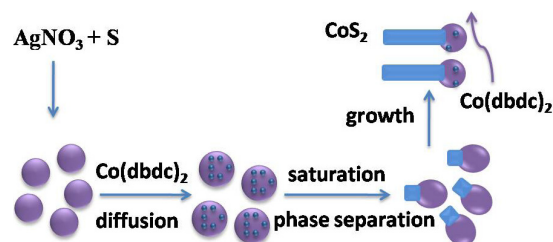
Co(dbdc)$_2$ must be slow. If the 120 mg of Co(dbdc)$_2$ was once poured into the reaction system, or with rate of 40 mg Co(dbdc)$_2$ every 5 min, separated Ag$_2$S and CoS$_2$ are obtained (Fig. S1, see Supporting Information). Quick adding of Co(dbdc)$_2$ would cause higher instantaneous concentration, which will cause self-nucleation, thus forming separated particles.

The formation mechanism of the Ag$_2$S–CoS$_2$ heterostructures is proposed. In the reaction system, spherical Ag$_2$S nanoparticles are first formed (Fig. 3(b)). Ag$_2$S is a superionic conductor, which has a high density of Ag$^+$ vacancies (or deficiencies), high cation mobility, and a nearly rigid sublattice of S^{2-} anions at a certain temperature.[23] Such unique structure features make the Ag$_2$S nanocrystal be like a liquid sphere. This feature is quite similar to that of a metal nanoparticle catalyst with low melt point used for the synthesis of semiconductor nanowires, and enables the excellent catalytic ability. Thus, the formed Ag$_2$S nanoparticles would be used as a unique catalyst for the growth of semiconductor. When Co(dbdc)$_2$ is introduced in the reaction system, the corresponding species will transport or diffuse into the Ag$_2$S nanoparticles till a saturation state is obtained. After that, CoS$_2$ phase separates out from Ag$_2$S host, forming a heterostructure with distinct interface. Then, Ag$_2$S nanoparticle takes in the cobalt species, which eventually separate out at the hetero-interface, inducing the growth of CoS$_2$ forming nanorods. This process is quite similar to the vapor–liquid–solid mechanism.[24,25] The curved hetero-interface with arc shape would relate to the interface (surface) energy that is affected by the mismatch strain.[24,25] Usually, a unique interface shape corresponding to a lower surface energy is dominant in the sample. Controlled experiment also shows that without Ag$_2$S in the reaction system, only irregular nanoparticles are obtained. This further suggests that the formation of one dimensional CoS$_2$ is with the assistance of Ag$_2$S. Scheme 1 exhibits the schematic growth process.

CoS$_2$ is a metallic ferromagnet with a curie temperature of about 120 K. We then preliminary studied the magnetic properties of the obtained Ag$_2$S–CoS$_2$ hetero-structures. zero field-cooled (ZFC) and field-cooled (FC) magnetization recorded on the Ag$_2$S–CoS$_2$ hetero-structures are demonstrated in Fig. 4(a). From the ZFC–FC curve, the hetero-structures

Fig. 3. (a) TEM image of Ag$_2$S–CoS$_2$ hetero-structure obtained with 50 mg of Co(dbdc)$_2$. (b) TEM image of Ag$_2$S nanoparticles.

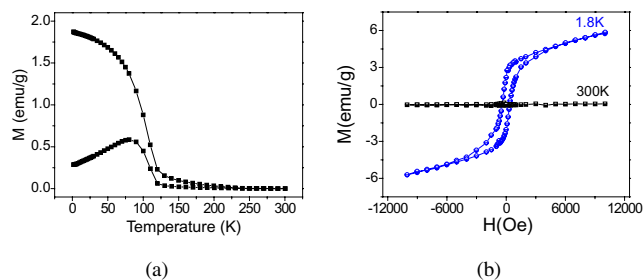Scheme 1. The growth process of the Ag$_2$S–CoS$_2$ hetero-structures.

Y. Liu et al.

(a) (b)

Fig. 4. (a) Temperature dependence of FC and ZFC curves of the Ag_2S–CoS_2 hetero-structures with magnetic field of 100 Oe. (b) M–H curves of the Ag_2S–CoS_2 hetero-structures measured at 1.8 K and 300 K.

show a clear evidence for ferromagnetic-paramagnetic transition with Tc *ca.* 120 K. This is consistent with the reported value for CoS_2.[26,27] Figure 4(b) shows the M–H curves measured at 300 K and 1.8 K. Typical paramagnetic properties can be observed at 300 K, and a well defined hysteresis loop with coercivity of 385 Oe is detected at 1.8 K, further demonstrating the ferromagnetism feature of the Ag_2S–CoS_2 hetero-structures below the transferring temperature. It should be noted that the magnetization of the hetero-structures at 1.8 K is 5.8 emu/g with a magnetic field of 10,000 Oe. Increasing the magnetization field to 80,000 Oe (Fig. S2, see Supporting Information), the magnetization curve tends to saturation and a saturation magnetization of 8.3 emu/g is obtained at 1.8 K. Considering that there is nonmagnetic Ag_2S composition in the sample, the actual saturation magnetization for CoS_2 in the hetero-structures is much higher.

Generally, the magnetization of ferromagnetic nanoparticles decreases with decreased diameter, because the ratio of surface disordered spins to internal ordered spins increases with the decreasing diameter. In our case, owing to the relatively smaller size, the saturation magnetization is lower than that of sub-micron or bulk CoS_2 ($\sim$ 30–40 emu/g).[28–31] While, the saturation magnetization value is quite higher than the reported value for CoS_2 nanoparticles with size of 20–60 nm (0.2 emu/g),[27] and is similar to CoS_2 octahedron particles with size of > 120 nm (12.8 emu/g).[28] It is difficult to understand this higher saturation magnetization at present stage. The formation of hetero-interface would cause the increase of magnetization. Owing to the stronger coupling interaction, Ag_2S phase would induce the increase of magnetization of CoS_2 through hetero-interface. Secondly, recent theoretical calculations and experimental observations[33–35] indicate that point defects can contribute magnetism. In our case, intrinsic defects on the surface or the interface would induce unpaired spin electrons that are prompted to a higher energy orbital enabling it to participate in the long-range magnetic order.

In summary, Ag_2S–CoS_2 hetero-structures were synthesized through a catalytic growth route, in which Ag_2S nanoparticles with superionic conductor properties play a catalyst role, inducing the growth of CoS_2. The Ag_2S–CoS_2 hetero-structures have well defined and sharp hetero-interface. In addition, the magnetic properties of the obtained Ag_2S–CoS_2 hetero-structures were investigated. The transition temperature of paramagnetic-ferromagnetism is consistent with the previous results of CoS_2. It is believed that the reported results would give some hints to the development of multifunction magnetic materials.

References

1. C. M. Donega, *Chem. Soc. Rev.* **40**, 1512 (2011).
2. M. Casavola *et al.*, *Eur. J. Inorg. Chem.* **6**, 837 (2008).
3. R. D. Robinson *et al.*, *Science* **317**, 355 (2007).
4. H. McDaniel *et al.*, *J. Am. Chem. Soc.* **132**, 3286 (2010).
5. K. P. Acharya *et al.*, *J. Phys. Chem. C* **114**, 12496 (2010).
6. L. D. Trizio *et al.*, *ACS Nano* **7**, 3997 (2013).
7. L. Carbone *et al.*, *Nano Today* **5**, 449 (2010).
8. W. Han *et al.*, *J. Am. Chem. Soc.* **130**, 13152 (2008).
9. G. X. Zhu *et al.*, *J. Am. Chem. Soc.* **133**, 148 (2011).
10. S. T. Connor *et al.*, *J. Am. Chem. Soc.* **131**, 4962 (2009).
11. B. Sadtler *et al.*, *J. Am. Chem. Soc.* **131**, 5285 (2009).
12. M. D. Regulacio *et al.*, *J. Am. Chem. Soc.* **133**, 2052 (2011).
13. T. T. Zhuang *et al.*, *Chem. Comm.* **48**, 9762 (2012).
14. X. F. Qian *et al.*, *Inorg. Chem.* **38**, 2621 (1999).
15. A. Wold *et al.*, *J. Solid State Chem.* **96**, 53 (1992).
16. B. Morris *et al.*, *J. Phys. Chem. Solids* **28**, 1565 (1967).
17. P. J. Brown *et al.*, *J. Phys. Condens. Matter.* **17**, 1583 (2007).
18. C. Zhao *et al.*, *J. Mater. Chem. A* **1**, 5741 (2013).
19. J. S. Jirkovsky *et al.*, *J. Phys. Chem. C* **116**, 24436 (2012).
20. P. J. Masset *et al.*, *J. Power Sources* **178**, 456 (2008).
21. C. Z. Yuan *et al.*, *J. Electrochem. Soc.* **156**, A199 (2009).
22. D. C. Pan *et al.*, *J. Am. Chem. Soc.* **130**, 5620 (2008).
23. S. Hoshino, *Solid State Ionics* **48**, 179 (1991).
24. N. Wang *et al.*, *Mater. Sci. Eng. R* **60**, 1 (2008).
25. J. Wallentin *et al.*, *Nano Lett.* **10**, 4807 (2010).
26. H. Nishihara *et al.*, *J. Phys. Conf. Series* **400**, 032068 (2012).
27. M. Lei *et al.*, *Mater. Lett.* **76**, 87 (2012).
28. J. T. Han *et al.*, *Mater. Lett.* **60**, 1805 (2006).
29. S. Miyahara *et al.*, *J. Appl. Phys.* **39**, 896 (1968).
30. S. Hebert *et al.*, *J. Appl. Phys.* **114**, 103703 (2013).
31. B. Liu *et al.*, *Mater. Lett.* **65**, 2804 (2011).
32. H. Hiraka, *J. Phys. Soc. Jpn.* **65**, 3740 (1996).
33. G. X. Zhu *et al.*, *J. Am. Chem. Soc.* **133**, 15605 (2011).
34. P. Dev *et al.*, *Phys. Rev. Lett.* **100**, 117204 (2008).
35. B. Song *et al.*, *J. Am. Chem. Soc.* **131**, 1376 (2009).